Environ. Sci. Technol. **2002**, *36,* 445−452

Is Silica Really an Anomalous Oxide? Surface Acidity and Aqueous Hydrolysis Revisited

NITA SAHAI*

Department of Geology and Geophysics, University of Wisconsin, Madison, Wisconsin 53706

The single-site **S**olvation, **B**ond Strength, and **E**lectrostatic (SBE) model accounts for the anomalous position of silica on the surface acidity versus aqueous acidity correlation developed for metal oxides, by considering the solvation energy change in the protonation reaction implemented through the dielectric constant ($1/\epsilon_k$) and the electrostatic energy change through the Pauling bond strength to bond length ratio (s/r) of the oxide. I address here why inclusion of the solid's dielectric constant brings silica into the same correlation as other oxides like TiO_2, Al_2O_3, and Fe_2O_3. The solvation and electrostatic contributions are interpreted in terms of classical concepts such as chemical hardness, polarizability, ionicity, electronegativity, and local charge densities. Silica is acidic (PZC < 7), not because of its small dielectric constant, its tetrahedral coordination, or its high bond strength alone. Surface acidity depends largely on high values of the s/r ratio. The dielectric constant of the solid affects acidity mainly by reflecting the nature of water−surface interactions. Solids with large values of ϵ_k are interpreted as being less polarizable and more ionic so that water, a hard polar solvent, interacts favorably with such surfaces and scales similar to water−water interactions regardless of whether the metal−oxide bond is in the solid or in the aqueous state. For these oxides, $pK_a^s = pK_a^{aq} \pm 1$. Silica, with a small dielectric constant, is interpreted as being more polarizable and more covalent so that water−SiO_2 interactions scale differently than for the more ionic oxides. Such an interpretation when combined with the Partial Charge Model for metal hydrolysis suggests that the surfaces of RuO_2, WO_3, Sb_2O_5, and Ta_2O_5 should be acidic similar to silica. But, unlike silica, they would lie on the pK_a correlation defined by the other oxides because of their larger dielectric constants. The mixed oxide, $AlPO_4$, is predicted to behave like silica.

1.0. Introduction

Attempts to rationalize the acidity of metal oxide surfaces, measured by the surface deprotonation constant (pK_a^s) and the point of zero charge (PZC), often rely on relating pK_a^s to the hydrolysis constant (pK_a^{aq}) of the metal ion in aqueous solution, where p = −log. A linear correlation has been suggested, $pK_a^s = pK_a^{aq} \pm 1$ (*1*). Because pK_a^{aq} can be correlated to z/r or s/r, attempts have been made to ultimately correlate pK_a^s or PZC with z/r or s/r, where z is the valence of the metal, s is the Pauling bond strength of the metal (*2*), and r is the metal−oxygen or metal−(O)H bond length (*3*−*7*). Silicon invariably occupies an "anomalous" position on such correlations in that the solid silica surface is much more acidic than expected from the 1:1 correlation with the pK_a^{aq} of silicic acid (*8, 9*) (Figure 1). Silica is also unusual in the shape of its surface charge (σ_0) vs (pH_{PZC}−pH) curve (*12*). The curve has a shallow slope up to ∼4 pH units above the PZC of silica as compared to other oxides, which have steeper slopes within 1−2 pH units from the PZC (Figure 2). Furthermore, the adsorption affinity sequence of monovalent cations on silica is $TMA^+ > Cs^+ > NH_4^+ > K^+ > Li^+$. This sequence is reversed from what is expected based on charge to radius ratio arguments, which appear to work for other oxides such as TiO_2, Al_2O_3, and Fe_2O_3 (*18*−*24*).

The **S**olvation, Pauling **B**ond Strength and **E**lectrostatic (SBE) model corrects for the anomalous position of silica on pK_a^s−pK_a^{aq} correlations by incorporating the change in solvation energy during sorption via a dielectric continuum approach (*8, 9*). The dielectric constant of the solid (ϵ_k) now becomes an additional parameter in the model, along with the Pauling bond strength per bond length (s/r). The related **S**olvation and **E**lectrostatic (SE) model predicts correctly the reversed affinity sequence for quartz based on the dielectric constant of the solid and the charge to radius ratio of the sorbing ion (*22*−*24*). The SBE/SE model is phenomenological, based on classical thermodynamics and electrostatic theory. The dielectric constant is a physical electrostatic property, and attempts have been made in the literature to interpret the SBE model on a molecular level using molecular dynamics simulations (*25, 26*), but the model was misunderstood. It would be useful to interpret the significance of the dielectric constant in the SBE model and, in fact, the entire model in a more chemically intuitive way.

The aim of this paper is to provide a heuristic interpretation of the SBE model. Four main issues will be addressed: (i) how and why inclusion of the solid's dielectric constant brings SiO_2 into the same correlation as other oxides, (ii) why pK_a^s and pK_a^{aq} of oxides correlate with s/r or z/r in the first place, (iii) the reason for the different curvature of surface charge vs (pH_{PZC}−pH) curves of different oxides, and (iv) the basis for ion adsorption affinity sequences. The model is reviewed briefly in Section 2 in order to define nomenclature. Section 3 provides a term-by-term order-of-magnitude analysis to determine which parameters contribute dominantly to surface acidity, followed by a comparison of the SBE model to some other phenomenological models (*27*−*31*). SBE model parameters are interpreted in terms of classical chemical concepts in Section 4 and are then combined with the Partial Charge Model (PCM) for aqueous metal hydrolysis to provide an intuitive understanding.

2.0. Review of SBE Model for Surface Protonation

Adsorption of protons at neutral (>SOH) and negatively charged sites (>SO^-) on the surface of the kth solid may be represented as

$$>SOH + H^+ \rightleftharpoons SOH_2^+ \qquad K_{a1}^s \qquad (1)$$

and

$$>SO^- + H^+ \rightleftharpoons SOH \qquad K_{a2}^s \qquad (2)$$

where the symbol ">" implies that the surface atoms are attached to the underlying bulk solid, the superscript "s" denotes a surface reaction. K_{a1}^s and K_{a2}^s are the associated equilibrium constants. Focusing on eq 2, the related Gibbs free energy of reaction ($\Delta G^\circ_{ads,H^+}$) may be expressed as the

* Telephone: (608)262-4972; fax: (608)262-0693; e-mail: sahai@geology.wisc.edu.

10.1021/es010850u CCC: $22.00
Published on Web 01/04/2002

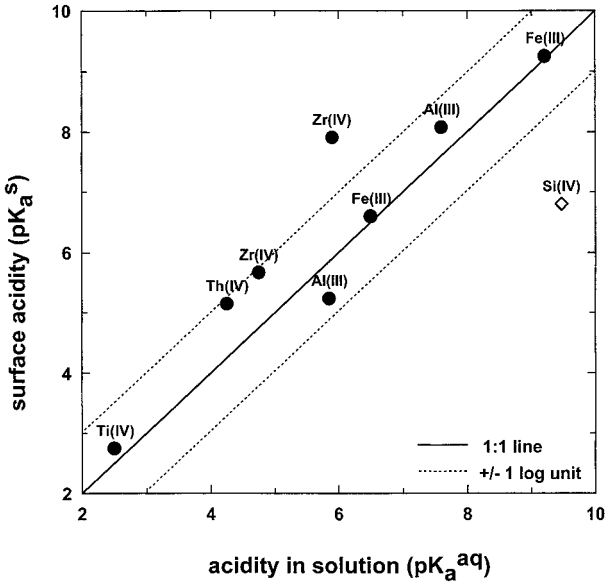

FIGURE 1. Correlation of surface acidity constants (pK_a^s) with aqueous hydrolysis/acidity constants (pK_a^{aq}), where p = −log (after Figure 4.7 of ref *1*). For Si(IV), pK_a^s = 6.8 (*10*) and pK_a^{aq} = 9.47 (*11*).

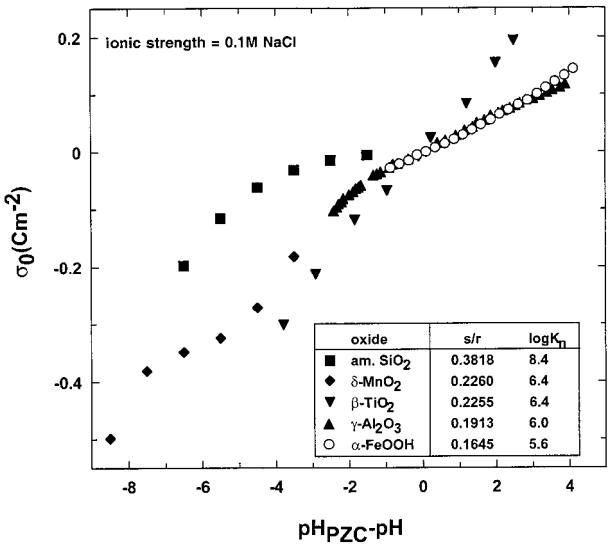

FIGURE 2. Surface charge (σ_0) vs pH$_{PZC}$−pH plot showing unusual shape of curve for SiO$_2$. The experimental data were collected from the literature: amorphous silica (*13*), δ-MnO$_2$ (*14*), β-TiO$_2$ (*15*), γ-Al$_2$O$_3$ (*16*), and α-FeOOH (*17*). All curves represent titrations at ionic strength set by 0.1 M NaCl background electrolyte. Values of log K_n calculated using eq 18. See section 4.3 of text for explanation.

sum of two contributions: (i) $\Delta G^\circ_{solv,H^+}$, the change in free energy of solvation for both the solid and the ion, and (ii) $\Delta G^\circ_{nonsolv,H^+}$, the free energy change due to effects not associated with solvation (*32, 8, 9*). Thus, the free energy of adsorption may be written as

$$\Delta G^\circ_{ads,H^+} = \Delta G^\circ_{solv,H^+} + \Delta G^\circ_{nonsolv,H^+} \quad (3)$$

Born solvation theory can be used to calculate charge-induced dipole (polarization) interactions (*33*), where the charge is due to the H^+ ion and the polarization is induced in different continuum media. The media are the solid, the interfacial region, and bulk water represented by their respective static, spatially averaged dielectric constants (ϵ_k, ϵ_{ifc}, ϵ_w), such that

$$\Delta G^\circ_{ads,H^+} = f_1\left(\frac{1}{\epsilon_k}\right) + f_2\left(\frac{1}{\epsilon_{ifc}}\right) + f_3\left(\frac{1}{\epsilon_w}\right) + \Delta G^\circ_{nonsolv,H^+} \quad (4)$$

in which f_1−f_3 denote different functions as detailed in the original development of the model (*9*). The nonsolvation term can be separated out into a contribution arising from electrostatic interaction between the proton and the surface oxygen (ΔG°_{pi}) and a term due to any other effects (ΔG°_{other}) such as van der Waal's forces, H-bonding of water molecules to the surface, and covalent bonding contributions. Thus, eq 4 may be written as

$$\Delta G^\circ_{ads,H^+} = f_1\left(\frac{1}{\epsilon_k}\right) + f_2\left(\frac{1}{\epsilon_{ifc}}\right) + f_3\left(\frac{1}{\epsilon_w}\right) + \Delta G^\circ_{pi} + \Delta G^\circ_{other} \quad (5)$$

ΔG°_{pi} can be further split up into two parts, $\Delta G^\circ_{atr,H-O}$ and $\Delta G^\circ_{rep,H-M}$, where ΔG°_{atr} is an attractive potential between the unit positive charge on the H^+ and the negative charge on the surface oxygen. $\Delta G^\circ_{rep,H-M}$ is a repulsive potential between the positively charged H^+ and the positively charged metal ion underlying the surface oxygen. So, eq 5 now becomes

$$\Delta G^\circ_{ads,H^+} = f_1\left(\frac{1}{\epsilon_k}\right) + f_2\left(\frac{1}{\epsilon_{ifc}}\right) + f_3\left(\frac{1}{\epsilon_w}\right) + \Delta G^\circ_{atr,H-O} + \Delta G^\circ_{rep,H-M} + \Delta G^\circ_{other} \quad (6)$$

The charge on the oxygen atom is fixed at −2 for all solids. Therefore, the $\Delta G^\circ_{atr,H-O}$ term is a constant for all oxides. The effective charge on the underlying metal atom can be estimated from the Pauling bond strength of the metal atom in the oxide (*2*):

$$s = \frac{\text{valence}}{\text{coordination number}} \quad (7)$$

Using electrostatic theory for the repulsive potential between H^+ and M^{s+}, it can be shown that the $\Delta G^\circ_{rep,H-M}$ term depends on s/r, where r is the length of the metal−(O)H bond. The parameter, s/r, varies with the solid. The free energy of adsorption thus becomes

$$\Delta G^\circ_{ads,H^+} = f_1\left(\frac{1}{\epsilon_k}\right) + f_2\left(\frac{1}{\epsilon_{ifc}}\right) + f_3\left(\frac{1}{\epsilon_w}\right) + f_4\left(\frac{s}{r}\right) + \Delta G^\circ_{atr,H-O} + \Delta G^\circ_{other} \quad (8)$$

in which f_4 denotes a function as detailed in the original development of the model (*9*). Attempts have been made to measure or estimate the value of the dielectric constant in the interfacial region by gas-phase adsorption of water on oxide surfaces, and low values of 3−6 are often obtained (*34*−*40*). But it is difficult to know how to relate those values obtained for water vapor to the value of ϵ_{ifc} for solids in liquid water. So, for convenience, the terms involving $1/\epsilon_{ifc}$ and other effects are lumped together into a separate factor within the curly brackets in eq 9. In doing this, it is assumed that the terms involving $1/\epsilon_{ifc}$ can be treated as constants. The $\Delta G^\circ_{atr,H-O}$ term is also included in curly brackets because it is a constant for all oxides, yielding

$$\Delta G^\circ_{ads,H^+} = f_1\left(\frac{1}{\epsilon_k}\right) + f_4\left(\frac{s}{r}\right) + \left\{f_2\left(\frac{1}{\epsilon_{int}}\right) + f_3\left(\frac{1}{\epsilon_w}\right) + \Delta G^\circ_{atr,H-O} + \Delta G^\circ_{other}\right\} \quad (9)$$

This results in the final form of the equation:

$$\Delta G^\circ_{ads,H^+} = c_1\left(\frac{1}{\epsilon_k}\right) + c_2\left(\frac{s}{r}\right) + c_3 \quad (10)$$

TABLE 1. Reference Table for Nomenclature Used in Present Paper As Compared with the Nomenclature Used in the Original Development of the SBE Model (*8, 9*) and the original MUSIC Model (*6, 7*)[a]

present nomenclature	original SBE model	MUSIC model
ΔG_{pi}°	$\Delta G_{pi,\nu}^{\circ}$	ΔG_{coul}°
ΔG_{other}°	$\Delta G_{ii,\nu}^{\circ}$ (ion-intrinsic term)	ΔG°*
$\left\{ f_2(1/\epsilon_{ifc}) + f_3(1/\epsilon_w) + \Delta G_{atr,H-O}^{\circ} + \Delta G_{other}^{\circ} \right\}$	$\Delta G_{ii,\nu}^{\circ\prime\prime\prime}$	

[a] The subscript ν refers to the type of protonation reaction (*9*), e.g., ν = 1, 2, PZC, and *n* for the reactions represented by eqs 1, 2, 13, and 16 of the present paper.

where c_1-c_3 are constants whose values are determined by calibration to experimental data. Equation 10 can be expressed in terms of the equilibrium constant (log K_2^s) corresponding to $\Delta G_{ads,H+}^{\circ}$. The calibration to experimental data consistent with the diffuse double-layer model (DDLM) yields numeric values for the functions c_1-c_3, resulting in (*9*)

$$\log K_2 = 11.07\frac{1}{\epsilon_k} - 18.49\frac{S}{r} + 12.27 \qquad (11)$$

and where triple-layer model (TLM) data were used, the regression obtained was (*9*)

$$\log K_2 = 21.1158\frac{1}{\epsilon_k} - 36.5688\frac{S}{r} + 16.4551 \qquad (12)$$

The preceding discussion was applied only to the situation where a proton adsorbs at a negatively charged site to produce a neutral site. The same considerations also apply to all other protonation levels of the surface. For instance, the reaction for the equilibrium constant at the zero point of charge of the oxide can be written as

$$>SO^- + 2H^+ \rightleftharpoons SOH_2^+ \qquad K_{PZC} \qquad (13)$$

Calibration of the corresponding equation on experimental data consistent with the DDLM yields (*9*)

$$\log K_{PZC} = 22.14\frac{1}{\epsilon_k} - 66.98\frac{S}{r} + 26.78 \qquad (14)$$

and calibration on experimental data consistent with the TLM yields (*9*)

$$\log K_{PZC} = 42.2316\frac{1}{\epsilon_k} - 85.8296\frac{S}{r} + 29.3732 \qquad (15)$$

The standard state chosen in the SBE/SE model for aqueous species is the hypothetical 1 molal solution referenced to infinite dilution. For surface species, the standard state is a 1 molal sorbed concentration and zero surface potential referenced to zero surface potential (*22*−*24*).

At the very outset, it is useful to note differences in terminology between the present paper and the original SBE model for surface protonation (Table 1). In the original work, for the νth protonation step where ν = 1, 2, *n*, or PZC, an "ion-intrinsic term" ($\Delta G_{ii,\nu}^{\circ}$) was defined as the sum of chemical bonding and all other factors (*8, 9*) by analogy with aqueous complexation theory (*41*). In aqueous complexes, the ion-intrinsic contribution refers to the fact that the identity of the metal ion changes from one complex to another. For adsorption of H^+, however, the identity of the adsorbing ion (H^+) is constant from one solid to another, so there is no inherent ion-intrinsic change. In the present paper, therefore, the ion-intrinsic label is avoided and is replaced by $\Delta G_{other,H+}^{\circ}$. In the original work, the $\Delta G_{ii,H+}^{\circ}$ term ended up in the $\Delta G_{ii,H+}^{\circ\prime\prime}$ term; the $\Delta G_{ii,H+}^{\circ\prime\prime\prime}$ term (*8, 9*) is identical to the term in curly brackets in eq 9 and to c_3 in eq 10 of the present paper.

3.0. SBE Model Analysis

3.1. Order of Magnitude Analysis. In eq 13, two protons are adsorbing instead of the single proton in eq 2. If our model is correct, then we should expect the value of $\Delta G_{atr,H-M}^{\circ}$ and $\Delta G_{rep,H-M}^{\circ}$ to be twice as large in eqs 14 and 15 as compared to their values in eqs 11 and 12. $\Delta G_{atr,H-O}^{\circ}$ is the dominant contributor to the c_3 term, and $\Delta G_{rep,H-M}^{\circ}$ is identified with the c_2 term in eqs 11 and 12. Therefore, the numeric values of c_2 and c_3 obtained by calibration on experimental data should be good indicators of the magnitudes of $\Delta G_{atr,H-O}^{\circ}$ and $\Delta G_{rep,H-M}^{\circ}$. The magnitudes of c_2 and c_3 (85.82, 29.37) in eq 15 are, indeed, almost twice their values in eq 12 (36.56, 16.45). Similarly, in eq 14, c_3 is 26.78 which is very close to twice the value of c_3 = 12.27, in eq 11. Only the value of c_2 (66.98) in eq 14 is large as compared to the value expected from eq 11 (2 × 18.49 = 37).

Subtracting eq 1 from eq 2 yields the reaction (*9*)

$$>SO^- + SOH_2^+ = 2{>}SOH \qquad \log K_n \qquad (16)$$

where log K_n = log K_{a2}^s − log K_{a1}^s. The lack of an explicit interaction between the surface oxygen and a proton approaching the surface from bulk solution suggests that the magnitude of the $\Delta G_{atr,H-O}^{\circ}$ term and the term in curly brackets in eq 9 should be small, i.e., c_3 should be small. Also, little or no dependence on ϵ_k should be expected. Calibration of the corresponding model equation on experimental data consistent with the DDLM and the TLM, respectively, yields

$$\log K_n = 30.01\frac{S}{r} - 2.238 \qquad (17)$$

and

$$\log K_n = 12.692\frac{S}{r} + 3.537 \qquad (18)$$

It can be seen eqs 17 and 18 that the c_3 term is indeed small (2.238, 3.537) and the equations are independent of ϵ_k. This analysis shows that, in general, our expectations based on electrostatic arguments are satisfied, suggesting that the SBE model reflects much of the underlying physics and chemistry involved in surface protonation.

The remaining terms in the model equations contain the parameters ϵ_k and s/r. Values of ϵ_k and s/r for many oxides and silicates are tabulated elsewhere (*8*−*9, 42*). The value of s/r varies between 0.1070 and 0.3818 Å^{-1} for oxides from MgO to quartz, so that the electrostatic repulsion term is an important contribution to $\Delta G_{ads,H+}^{\circ}$. The term in curly brackets, dominated by $\Delta G_{atr,H-O}^{\circ}$, is of comparable magnitude. The term containing $1/\epsilon_k$ is the smallest contribution to the adsorption energy for most, but not all, oxides.

3.2. Implications of Obtaining a Constant Value for $\Delta G_{ii,H^+}^{\circ\prime\prime}$. It is curious that $\Delta G_{ii,H^+}^{\circ\prime\prime}$ can be treated as constant for all oxides (*8, 9*) because it contains the $1/\epsilon_{ifc}$ term, and it is reasonable to expect that the structure of interfacial water varies from one surface to another. On the basis of such reasoning, it was suggested that a verifiable corollary of the SBE model is that gas-phase deprotonation energies ($\Delta E_{g,dp}$) of protons on oxide surfaces should correlate with the solution-phase surface acidities (*25*). The authors were, however, unable to identify positively charged silica species in the gas-, solution- and surface-phase using molecular static calculations. Their attempt to predict pK_a^{aq} of $H_5SiO_4^+$

TABLE 2. Comparison of Model Parameters and Calculated PZC Values with Experimental Values[a]

oxide	valence	CN	r_{M-O}[b,c] (Å)	s/r_{M-H}[d] (Å^{-1})	ϵ_k[e]	PZC (calcd)[f]	PZCs (expt)[g]
α-SiO_2	IV	4	1.61 (*8*)	0.3818 (*8*)	4.578	2.91 (*8*)	2.9 (*8*)
WO_3	VI	6 (*46*)	1.94	0.3390	(?) ∼35[h]	0.74	0.3−0.5, 1.5, ∼5 (*3*, *48*−*52*)
MoO_3	VI	6	2.09	0.3236			1.8−2.1 (*53*)
Sb_2O_5	V	6	2.0	0.2769			1.9 (*49*)
Ta_2O_5	V	6	2.04	0.2732	45.0	3.43	2.9 (*50*, *54*)
Nb_2O_5	V	6	2.04	0.2732	38.0	3.52	∼4 (*49*)
β-MnO_2, pyrolusite	IV	6	1.89 (*55*)	0.2300	10 000 (*8*)	4.77	4.6−7.3 (*8*, *50*, *56*−*59*)
δ-MnO_2, vernadite	IV	6	1.94 (*55*)	0.2260			1.5−2.15 (*14*, *50*, *56*−*59*)
RuO_2	IV	6	2.02	0.2200			4−6 (*59*−*61*)
Cr_2O_3	III	6	1.7	0.1845	12.3	8.48	7.0 (*3*)
Al_2O_3	III	6	1.90 (*8*)	0.1711 (*8*)	10.43	9.37 (*8*)	8.1−8.4 (*50*) (γ-Al_2O_3), 9.8−9.1 (*8*, *50*) (α-Al_2O_3)
Sb_2O_3	III	6	2.0 (*46*)	0.1661	8.2	10.13	
V_2O_3, karelianite	III	6	2.04	0.1645	∼15.0 (*62*)	9.03	8.4 (*63*)
Y_2O_3	III	6	2.30	0.1645	11.3	9.50	8.6−9.0 (*5*, *49*, *63*)
MgO	II	6	2.10 (*8*)	0.1070 (*8*)	9.83	12.24 (*8*)	12.4 (*3*)

[a] Arranged in order of decreasing s/r. Many of the metal−oxygen bond lengths are estimates, so the predicted PZCs are only approximate values and are shown here more for a heuristic benefit than for a desire for numerically accurate prediction. [b] r_{M-O} is the average metal−oxygen bond length. Ideally, this distance should be obtained from crystal structures of the oxides. Lacking such information in some cases, r_{M-O} has been estimated as r_{M-O} ∼ metal ionic radius +1.4 Å (radius of oxygen) where. [c] Shannon ionic radius used (*45*), unless noted otherwise. [d] $r_{M-H} = r_{M-O} + 1.01$ (1.01 Å is the O−H distance in ice). [e] From ref *42*, unless noted otherwise. [f] PZC values were calculated using the SBE model equation: $PZC = 21.1158(1/\epsilon_k) - 42.9148(s/r_{M-H}) + 14.6866$ (*8*). [g] No distinction is made here between "pristine" points of zero charge, common intersection points of acid−base titration curves at different ionic strengths, and isoelectric points. [h] Estimated from Figure 1 of *47*.

using a correlation of pK_a^{aq} with $\Delta E_{g,dp}$ of Fe(III) hydroxo and $H_4SiO_4/H_3SiO_3^-$ clusters resulted in too large a value of 4.9. These results were used to question the validity of the SBE model.

There are several problems with such conclusions. First, the idea that ϵ_{ifc} is constant with suggested values of ∼3−6 and ∼40 is not new and has precedence in independent experimental and modeling studies (*34*−*40*, *43*). Actually, the SBE model does not necessarily require ϵ_{ifc} to be constant just because $\Delta G^{\circ\prime\prime}_{ii,H^+}$ is constant. The order of magnitude analysis in section 3.1 shows that $\Delta G^{\circ\prime\prime}_{ii,H^+}$ is dominated by $\Delta G^{\circ}_{atr,H-O}$, and contributions due to variations in ϵ_{ifc} are minor so the resulting effect on $\Delta G^{\circ\prime\prime}_{ii,H^+}$ should be negligible. The ϵ_{ifc} term may vary, but solvation energy depends on $1/\epsilon_{ifc}$, so even an order of magnitude variation in ϵ_{ifc} would only change total adsorption energy by 10−15%. Further, the ΔG°_{pi} term of the SBE model refers to interaction between a surface site and a H^+ that are already in solution (see caption to Figure 1 of ref *9*). The $\Delta G^{\circ}_{solv,H^+}$ term refers to changes in solvation from solution to the surface (the lack of a gas to solution solvation change may be an oversight in the model, but it has apparently little effect on results). Thus, pairwise differences between $1/\epsilon_w$, $1/\epsilon_{int}$, and $1/\epsilon_k$ appear in the solvation energy term (*9*), but there is no corresponding gas to solution term for either H^+ or the surface. This explains why the corollary deduced in ref *25* that a constant value of $\Delta G^{\circ\prime\prime}_{ii,H^+}$ implies a correlation between gas-phase pK_a^s and solution-phase pK_a^s is not correct.

Finally, the failure to identify a positively charged silica species by molecular mechanics modeling is not sufficient proof that the species does not exist. A recent study based on ab initio calculations showed the existence of stable positively charged solvated clusters, $Si(OH)_3(H_2O)_4^{1+}$ and $Si(OH)_3(H_2O)_8^{1+}$ (*44*). The pK_a predicted for the closely related $Si(OH)_3(H_2O)^{1+}$ species was −5, which compares reasonably well with the −1.1 and −0.3 values from DDLM and TLM calibrations of the SBE model (*8, 9*) but is much different from the value of 4.9 obtained by molecular statics (*25*). The point is that at present time molecular modeling and ab initio studies have limited ability to model surfaces in solution, so it is premature to use such calculations to "verify" phenomenological models.

3.3. Implications of the Magnitude of the $1/\epsilon_k$ and s/r Terms. The inverse dependence on dielectric constant has an interesting consequence. For most solids, ϵ_k is large enough that the $1/\epsilon_k$ term is not a significant contribution, leaving the s/r term as the main variable determining pK_a^s. In general, the value of s/r and of $\Delta G^{\circ}_{atr,H-O}$ for a metal−oxygen bond is similar in both solid and aqueous phase. This explains how a satisfactory agreement is observed between pK_a^s and pK_a^{aq} for many metals such as Ti^{IV}, Fe^{III}, and Al^{III}. For quartz and amorphous silica with low values of ϵ_k, the $1/\epsilon_k$ term makes a significant contribution to pK_a^s, so if neglected, a poor agreement is obtained between pK_a^s and pK_a^{aq}.

It is useful to emphasize the different roles played in the SBE model by the $1/\epsilon_k$ and s/r terms. The local charge density represented by s/r mainly determines acidity: the larger the value of s/r, the more acidic is the metal oxide, where an acidic surface is defined as PZC < 7 and a basic surface as having PZC > 7. Thus, the high acidity of silica has little to do with a low value ϵ_k; other minerals such as δ-MnO_2, Ta_2O_5, and Nb_2O_5 (Table 2) also have low values of PZC even though they do not have low values of ϵ_k. Nor is the low PZC of silica related to the fact that silica is tetrahedrally coordinated; 5- and 6-fold coordinated metal oxides such as Ta_2O_5 and δ-MnO_2 are also highly acidic. Similarly, the SBE model predicts that magnetite and maghemite are both acidic because of their large values of s/r, not because they have similar values of Pauling bond strength (s) or because of their large values of $1/\epsilon_k$ as incorrectly stated in the literature (*26*). The value of ϵ_k determines, mainly, whether the surface and solution pK_a will correlate. If ϵ_k is large, the surface and solution pK_a will correlate almost 1:1. These ideas are illustrated by comparing Ta_2O_5 and Nb_2O_5 with silica. Larger values of ϵ_k for Ta_2O_5 and Nb_2O_5 (Table 2) ensure that the solvation contribution is small so that their pK_a^s should be similar to pK_a^{aq} (±1 log unit), despite their highly acidic surfaces.

3.4. Validity of Electrostatic Models. The idea that an electrostatic potential does not capture the "specific" or covalent part of the system (*64*) is not entirely accurate. The s/r term represents molecular structures through Pauling's rules making it an inherently coordination chemistry approach (*65*) and represents specificity of the metal through the metal−oxygen bond length. An extended ionic approach where ions have formally assigned charges may be used effectively to explain conventionally defined covalent properties of crystalline solids, where covalent is defined as

"anything not predicted by the simplest ionic picture" (*66, 67*). Recent ab initio molecular orbital (MO) studies have also found that acidities of oxyacid monomers, oligomers and surfaces are dominated by local electrostatic contributions (*44, 68*), and formal charges on the monomers performed better than partial charges derived from sophisticated molecular orbital overlap calculations (*44*). Gas-phase acidities of monomers can be related to the degree of underbonding ($2 - s_i$) at the oxygen site, where s_i is the Brown bond strength (*31*) that contains a built-in distance parameter (*30, 44*). The MO study also found greater acidity with increasing oligomerization as compared to the monomer, H_4SiO_4, and concomitant shortening of the Si−O bond resulting in a decreasing magnitude of $2 - s_i$ (*44*). Moreover, constants c_1−c_3 in eqs 11, 12, 15, 17, and 18 have magnitudes expected from electrostatic theory (section 3.1). Thus, electrostatic models can do a resonable job of estimating surface acidity of oxides. Finally, inclusion of ϵ_k indirectly builds in an extra parameter for capturing nonelectrostatic effects, through the polarizability (see section 4 below).

3.5. Comparison with the MUSIC Model. The SBE and MUSIC models are similar in that they both rely on classical electrostatic theory to account for the attractive and repulsive forces between the adsorbing proton and the oxygen or metal atoms constituting the surface site. The ΔG°_{pi} and ΔG°_{other} terms in eq 5 may be identified with the ΔG°_{coul} and $\Delta G^{\circ *}$ terms of the MUSIC model (*6, 7*) (Table 1). In the SBE model, the charge on the surface oxygen of all solids is restricted to −2 by definition, resulting in a single-site model. In a real system, the proton probably does not experience the entire −2 charge on the surface oxygen, which is bonded to metal atoms under the surface so that part of the −2 charge is already satisfied. The extent of residual charge or degree of under-bonding of the oxygen atom is $(-2 + ns)$, where n is the number of metal atoms coordinating the oxygen atom and s is the Pauling bond strength. This approach leads to a multisite model (*27*−*29*). Alternatively, the Brown bond-valence can be used, and it contains a built-in distance parameter (*30, 31*). All these models attempt to estimate the local charge density on the surface atoms.

A major difference between the SBE and the original MUSIC model is that solvation changes are neglected in the latter. The modified MUSIC model now includes solvation by explicit ad hoc accounting of H-bonds donated to or accepted by surface sites for each solid (*27*). The SBE model is based on a thermodynamic, continuum dielectric approach whereas the modified MUSIC model depends on explicit hydration, analogous to the continuum solvation models versus the explicit water molecules (supermolecule) approach used in quantum chemical cluster calculations. It is likely that both explicit and continuum solvation are necessary to accurately model solvation. Furthermore, the SBE model directly relates experimental values of pK_a^s to parameters of the solid such as s/r and ϵ_k. The MUSIC approach, on the other hand, relates pK_a^{aq} to s/r in solution and requires an additional step relating pK_a^{aq} to pK_a^s.

The MUSIC model has been used widely because of its multisite basis. The advantages and disadvantages of single- versus multisite models have been discussed elsewhere (*24*). Different models should be chosen for different purposes. At the same time, a multisite model is a more realistic representation, so the ideal model would combine a multisite approach with explicit and continuum solvation and would be directly calibrated on surface pK_a values. Such a model remains to be constructed.

4.0 Interpretation of the SBE Model

In section 3.3, we saw how the magnitude of $1/\epsilon_k$ primarily determines whether pK_a^s will correlate with pK_a^{aq}, and s/r mainly determines whether the solid will be acidic or basic. Here, we address why the dielectric constant of the solid affects surface hydration or why inclusion of ϵ_k brings silica into the same correlation as other oxides, and the reason for the reversed cation affinity sequence on silica. Next, metal acidities in solid and in solution phase will be examined. That is, why do pK_a^s and pK_a^{aq} correlate with s/r in the first place? Finally, the unusual surface charge versus pH_{PZC}−pH curve of silica will be interpreted.

4.1. Role of the Dielectric Constant. The dielectric constant is related to electric polarizability and molar volume through the Clausius−Mossotti equation (*42*). The electronegativity (χ) and absolute hardness (η) or extent of ionicity versus covalency of the metal−oxide bond is a rough measure of the chemical polarizability (*69, 70*) and, hence, of the dielectric constant if molar volume and ionic valence are ignored for the present. It has been noted previously in a qualitative way that as dielectric constant of a solvent medium decreases, the softness or polarizability of the medium increases (*71*). In our case, the medium is the solid oxide. Limited support for this concept is provided by the trends seen between ionicity and dielectric constant with parameters that roughly estimate the polarizability (Table 3 and Figure 3). ΔN is the ratio of the electronegativity difference between the metal and the oxygen, which drives electron transfer in a bond, and the hardness sum, which resists electron transfer (*70*). Thus, ΔN is a measure of the fraction of electrons transferred when a metal−oxygen bond is formed. A similar parameter where the denominator is the difference in hardness between metal and oxygen atoms also appears to relate to the ionicity and dielectric constant. ΔN correlates better with ionicity (Figure 3a,c) than with dielectric constant. The hardness difference parameter performs better with ϵ_k (Figure 3b,d). The trends in Figure 3 suggest that electronegativity and "hardness" capture some of the polarizability of a metal−oxide bond. At the same time, it is critical to remember that these are very rough approximations. The correlations fail to capture the difference between oxides of the same metal with a different valence such as Sb_2O_3 and Sb_2O_5, or the difference between polymorphs of the same oxide (the influence of molar volume on the dielectric constant) such as rutile and anatase, vernadite (δ-MnO_2) and pyrolusite (β-MnO_2), and quartz and amorphous silica. Thus, electric polarizability is not strictly synonymous with Pearson's original use of the term chemical polarizability nor with absolute hardness and absolute electronegativity, the HOMO−LUMO gap, electron affinity and ionization potentials, and the presence or absence of d-orbitals on the metal atom (*72*−*77*). Still, an "intuitive" understanding of the SBE model is afforded by a discussion of the chemical polarizability and ionicity versus covalency of metal−oxide bonds.

According to the Pauling electronegativity scale, the Si−O bond has about 50% ionic character, whereas the Ti−O, Fe−O, and Al−O bonds are relatively more ionic in character (*2, 78*), So, SiO_2 may be considered "softer" than these oxides, consistent with the trends in Figure 3. Water is a polar, hard solvent. The comparatively soft character of silica implies that interactions with water will scale differently than water−water interactions. On the other hand, interactions of water with more ionic solids will scale as water−water interactions, regardless of whether the metal−oxygen bond is in the solid or the aqueous state. This explains the linear correlation between the aqueous and the surface pK_a for oxides such as TiO_2, Fe_2O_3, and Al_2O_3 as compared to the "anomalous" position of SiO_2 in such correlations. It also explains why different correlation lines are required for different types of species such as iron hydroxo species as compared to the oxyacids of Si, As, P, etc. (*79*).

Similar arguments can be used to explain the reversed ion affinity sequence on SiO_2 using the SE model (*24*). The

TABLE 3. Relating Oxide Dielectric Constant to Different Measures of Polarizability, ΔN and $(\chi_{metal} - \chi_{oxygen})/(\eta_{metal} - \eta_{oxygen})$, in a Metal−Oxygen Bond[a]

atom	Mulliken electronegativity, χ[a]	absolute hardness, η[a]	ΔN[b] $= (\chi_{metal} - \chi_{oxygen})/2(\eta_{metal} + \eta_{oxygen})\}$	$(\chi_{metal} - \chi_{oxygen})/(\eta_{metal} - \eta_{oxygen})$	oxide	static dielectric constant, ϵ_k
Mn	3.72	3.72	−0.1949	1.6186	MnO_2	~10,000
Ti	3.45	3.37	−0.2164	1.5092	α-TiO_2	120.91
Ta	4.11	3.79	−0.1738	1.4978	Ta_2O_5	45
Nb	4	3.0	−0.1949	1.1494	Nb_2O_5	38.0
W	4.4	3.58	−0.1625	1.2560	WO_3	
Fe	4.06	3.81	−0.1759	1.5330	Fe_2O3	25
Ti	3.45	3.37	0.7456	1.5092	β-TiO_2	21.32
V	3.6	3.1	−0.2146	1.3221	V_2O_3	15
Cr	3.72	3.06	−0.2090	1.2649	Cr_2O_3	12.3
Ca	2.2	4.0	−0.2649	2.5673	CaO	12.01
Al	3.23	2.77	−0.2435	1.3021	Al_2O3	10.43
Mg	3.75	3.9	−0.1899	1.7385	MgO	9.83
Sn	4.3	3.05	−0.1774	1.0693	SnO_2	9
Sb	4.85	3.8	−0.1361	1.1798	Sb_2O_3	8.2
Ge	4.6	3.4	−0.1551	1.0970	GeO_2	6.5
Si	4.77	3.38	−0.1464	1.0259	SiO_2	4.578
Ru	4.5	3.0	−0.1674	0.9870	RuO_2	
Mo	3.9	3.1	−0.1983	1.2215	MoO_3	
O	7.54	6.08				

[a] Arranged in order of decreasing dielectric constant. [b] Table 3 of ref *70*. [c] ΔN is a measure of fractional electron transfer (*70*).

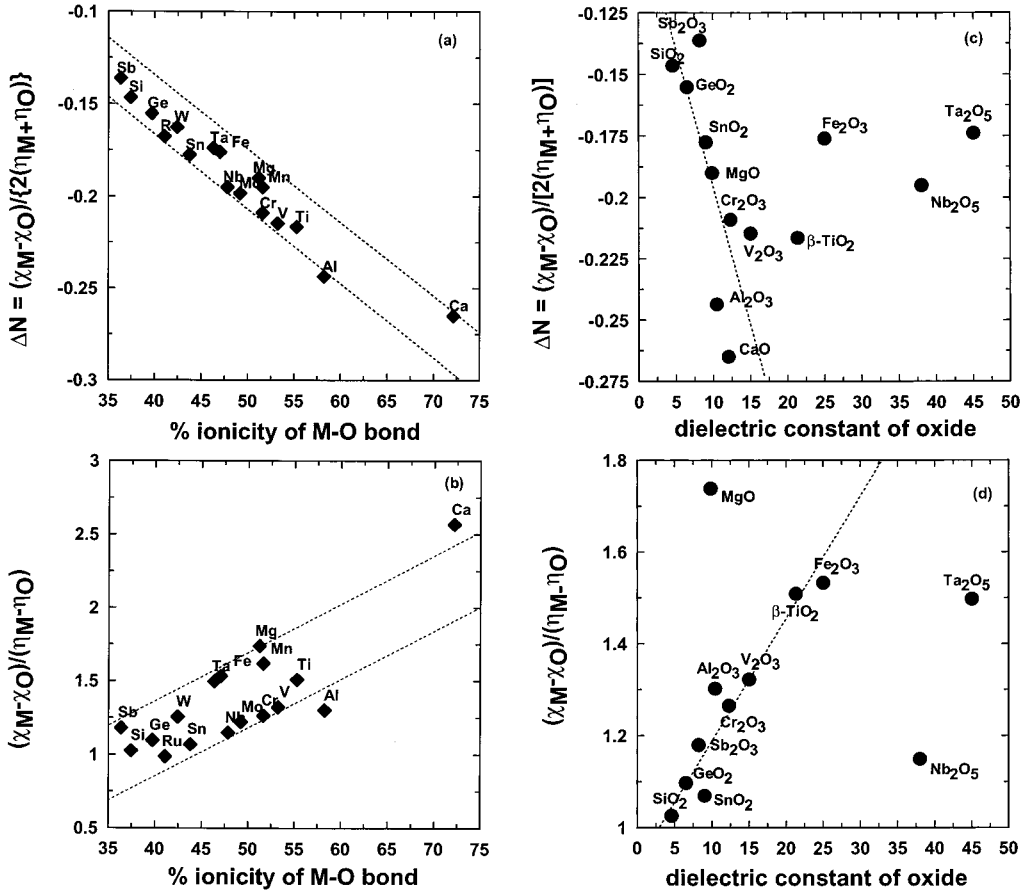

FIGURE 3. Approximate relationships between oxide dielectric constant and bond ionicity with different measures of polarizability in terms of electronegativity and hardness. The dashed lines are *not* best fit lines and are only meant to guide the eye.

softest hydrated alkali cation, Cs^+, and the SiO_2 surface interact more favorably than the harder hydrated Li^+ ion and SiO_2. The opposite is true for more ionic solids such as F_2O_3 and TiO_2. Interestingly, the model predicts that despite their acidic surfaces, the ion affinity sequences of RuO_2, WO_3, Sb_2O_3, Ta_2O_5, and Nb_2O_5 will follow the trends seen for TiO_2, Fe_2O_3, and Al_2O_3 because all these oxides have larger values of ϵ_k than SiO_2.

Points of zero charge and electrolyte ion affinity sequences have been explained previously in the literature using similar ideas involving polarity and electric field effects of oxides and structure-breaking and structure-making properties of oxide surfaces toward water (*18, 19, 56, 57, 80*). Thus, the SBE model builds on previous ideas and quantifies them within a thermodynamic framework.

4.2. Local Charge Density Interpretation of Acidities. The acidity of silica compared to basic oxides such as Fe_2O_3 and Al_2O_3 is also reflected in the aqueous state by the hydrolysis, condensation and aqueous complexation properties of Si^{IV} versus Fe^{III} and Al^{III}. Si^{IV} forms aqueous polyacids whereas Fe^{III} and Al^{III} form oxides and hydroxides. It is, then, reasonable to suggest a fundamental difference in the local character of the Si−O bond, regardless of whether the bonds are in the solid or aqueous state. To a first approximation, the local electronic structure is responsible for the observed difference. One can now ask if there any other metals or metalloids that behave like Si^{IV}.

The **P**artial **C**harge **M**odel (PCM) uses ionic valence and electronegativity to explain differences in hydrolysis, condensation, and aqueous complexation behavior of metal ions (*81*). The valence and electronegativity of the ion as compared to the electronegativity of H^+, OH^-, and H_2O are used to define classes of ions that form bases, hydroxides, polyacids, or acids in aqueous solution. The PCM predicts that Zr^{IV}, Mn^{IV}, Ti^{IV}, Ce^{IV}, Fe^{III}, Al^{III}, Cr^{III}, Mn^{II}, and Pb^{II} should form hydroxides and oxides. On the other hand, ions such as Ru^{IV}, W^{VI}, Mo^{VI}, Ta^{V}, and Sb^{V} belong to the same class as Si^{IV} and should form polyacids in aqueous solution (Figure 2 of ref *81*). Following the local electronic structure argument regardless of solid or aqueous state, solid RuO_2, WO_3, MoO_3, Ta_2O_5, Sb_2O_5, Nb_2O_5, and B_2O_3 should also have acidic surfaces similar to SiO_2. This prediction is consistent with observation. The discussion in section 4.1, however, indicates that the large values of ϵ_k for oxides such as RuO_2, WO_3, and Ta_2O_5, will result in their pK_a^s correlating with hydrolysis pK_a^{aq} similar to Ti^{IV}, Fe^{III}, and Al^{III}. As seen in Table 2, the PZCs predicted by the SBE model, the qualitative analysis of the SBE model in terms of the PCM, and experimental data are all in excellent agreement. A qualitative relation between surface acidity and electronegativity has been noted previously for oxides and sulfides (*3, 54, 82*). A caveat to the local charge density interpretation is that the effects of long-range forces and crystal structure have been neglected. Therefore, the acid−base behavior of solids and aqueous ions should not be expected to be consistent in all cases.

4.3 Shape of the Surface Charge (σ_0) vs pH_{PZC}−pH Curve. The shape of the curve shows the "rate" at which the concentration of charged surface sites increases and concentration of neutral sites decreases with increasing pH away from the PZC (although the neutral sites always dominate in total concentration). The steeper the curve, the greater the percentage of charged surface sites at a pH close to the PZC. Thus, the shape of the curve is a measure of the magnitude of K_{a2}^s/K_{a1}^s ratio or K_n (eq 16), which depends on s/r according to the SBE model (eqs 17 and 18). An oxide with a larger value of s/r should have a larger fraction of neutral sites at a given number of pH units from the PZC as compared to an oxide with a smaller value of s/r (see insert in Figure 2). The large values of s/r for WO_3 and MoO_3 (Table 2) suggest that these oxides will have σ_0 vs pH_{PZC}−pH curves similar to SiO_2. Vernadite is negatively charged like SiO_2, but the shape of the curve resembles β-TiO_2 because of similar s/r values. Similarly, γ-Al_2O_3 and α-FeOOH have similar s/r values and shape of the curve. The slope of the curves increases consistently for these sample pairs of oxides as their s/r values decrease. There is no dependence on ϵ_k because the proton is only moving from one surface site to another without significant solvation changes occurring.

4.4 Weird and One-of-a-Kind? So is silica anomalous? If considered simply in terms of acidic versus basic nature, it is not, because many other oxides such as δ-MnO_2, WO_3, MoO_3, RuO_2, and Ta_2O_5 are also acidic. Also, using the SBE model, oxides such as MoO_3 and WO_3 are predicted to behave like silica in terms of the shape of the surface charge curve but like the "well-behaved" oxides such as TiO_2 and Fe_2O_3 in terms of cation affinity sequence. Thus, there is spectrum of different types of behaviors that can be rationalized consistently for all the oxides using the SBE model. In this sense, silica is not so much anomalous as unusual. Are there other solids that behave like silica in all the surface properties discussed here or is silica unique? The mixed oxide $AlPO_4$ has a low dielectric constant of 4.55 (*42*) and large s/r of 0.3788 $Å^{-1}$ value (structure from *83*) similar to silica. If treated as a single-site model oxide, it is predicted that $AlPO_4$ will have an acidic surface with PZC = 3.1, a σ_0 vs pH_{PZC}−pH curve similar to silica, and a reversed ion affinity sequence.

5.0 Summary

Analysis of the SBE model suggests that the anomalous position of silica and quartz in pK_a^s vs pK_a^{aq} correlations and their reversed ion affinity sequence for monovalent cations are due to the low dielectric constant of the solids. Interpretation of results in terms of classical chemistry concepts such as ionicity, hardness, plarizability, local charge density, and electronegativity allows us to interpret the role of the dielectric constant in the SBE model as a measure of the water−water versus water−solid interactions. Analysis in terms of local charge densities highlights similarities in the acidity of metal−oxide bonds in solution and on surfaces and affords a modicum of consensus among the aqueous hydrolysis and surface acidity models in the literature.

Acknowledgments

This paper was inspired by discussions over the years with Prof. Alan Stone at Johns Hopkins University, Prof. Jim Morgan during his sabbatical leave at Johns Hopkins in the fall of 1996, Prof. Jack Tossell at University of Maryland−College Park, Dr. Jim Rustad of Pacific Northwest National Laboratory, and Dr. Suvasis Dixit at Georgia Tech. I am grateful for the constructive comments and criticisms of two anonymous reviewers and of the associate guest editor, Prof. Russ McDuff.

Literature Cited

(1) Schindler, P. W.; Stumm, W. In *Aquatic Surface Chemistry: Chemical Processes at the Particle−Water Interface*; Stumm, W., Ed; Wiley: New York, 1987; pp 83−110.
(2) Pauling, L. *The Nature of the Chemical Bond*, 3rd ed.; Cornell University Press: Ithaca, NY, 1960; Chapter 3.
(3) Parks, G. A. *Chem. Rev.* **1965**, *65*, 177.
(4) Tanabe, K.; Sumiyoshi, T.; Shibata, K.; Tadamitsu, K.; Kitagawa, J. *Bull. Chem. Soc. Jpn.* **1974**, *47*, 1064.
(5) Yoon, R. H.; Salman, T.; Donnay, G. *J. Colloid Interface Sci.* **1979**, *70*, 483.
(6) Hiemstra, T.; Wit, J. C. M. D.; Van Riemsdijk, W. H. *J. Colloid Interface Sci.* **1989**, *133*, 91.
(7) Hiemstra, T.; Wit, J. C. M. D.; Van Riemsdijk, W. H. *J. Colloid Interface Sci.* **1989**, *133*, 105.
(8) Sverjensky, D. A. *Geochim. Cosmochim. Acta* **1994**, *58*, 3123.
(9) Sverjensky, D. A.; Sahai, N. *Geochim. Cosmochim. Acta* **1996**, *60*, 3773.
(10) Schindler, P. von.; Kamber, H. R. *Helv. Chim. Acta* **1968**, *51*, 1781−1786.
(11) Sjöberg, S.; Öhman, L.-O.; Ingri, N. *Acta Chem. Scand.* **1985**, *A*39, 93.
(12) Lyklema, J.; Fokkink, L. G. J.; de Keizer, A. *Prog. Colloid Polym. Sci.* **1990**, *83*, 46.
(13) Bolt, G. H. *J. Phys. Chem.* **1957**, *61*, 1166.
(14) Balistrieri, L. S.; Murray, J. W. *Geochim. Cosmochim. Acta* **1982**, *46*, 1041−1052.
(15) Sprycha, R. *J. Colloid Interface Sci.* **1984**, *102*, 173.
(16) Huang, C.; Stumm, W. *J. Colloid Interface Sci.* **1973**, *43*, 409.
(17) Lumsdon, D. G.; Evans, L. J. *J. Colloid Interface Sci.* **1994**, *164*, 119.
(18) Berube, Y. G.; De Bruyn, P. L. *J. Colloid Interface Sci.* **1968**, *28*, 92.
(19) Eisenman, G. *Glass Electrodes for Hydrogen and Other Cations*; Mercel Dekker: New York, 1967; Chapter 7.
(20) Tadros, Th. F. *Discuss. Faraday Soc.* **1971**, *52*, 372.

(21) Dumont, F.; Watillon, A. *Discuss. Faraday Soc.* **197**1, *52*, 375−376.
(22) Sahai, N.; Sverjensky, D. A. *Geochim. Cosmochim. Acta* **1997**, *61*, 2801.
(23) Sahai, N.; Sverjensky, D. A. *Geochim. Cosmochim. Acta* **1997**, *61*, 2827.
(24) Sahai, N. *Geochim. Cosmochim. Acta* **2000**, *64*, 3629.
(25) Rustad, J. R.; Wasserman, E.; Felmy, A. R.; Wilke, C. *J. Colloid Interface Sci.* **1998**, *198*, 119.
(26) Rustad, J. R. In *Molecular Modeling Theory: Applications in the Geosciences*; Cygan, R. T., Kubicki, J. D., Eds.; Reviews in Mineralogy and Geochemistry 42; Mineralogical Society of America: Washington, DC, 2001; pp 190−191.
(27) Hiemstra, T.; Venema P.; Van Riemsdijk, W. H. *J. Colloid Interface Sci.* **1996**, *184*, 680.
(28) Hiemstra, T.; Van Riemsdijk, W. H. *J. Colloid Interface Sci.* **1999**, *210*, 182.
(29) Hiemstra, T.; Van Riemsdijk, W. H. *J. Colloid Interface Sci.* **1996**, *179*, 488.
(30) Bleam, W. F. *J. Colloid Interface Sci.* **1993**, *159*, 312.
(31) Brown, I. D.; Altermatt, D. *Acta Crystallogr. Sect. B* **1985**, *41*, 244.
(32) James, R. O.; Healy, T. W. *J. Colloid Interface Sci.* **1972**, *40*, 65.
(33) Israelachvili, J. *Intermolecular and Surface Forces*, 2nd ed.; Academic Press: London, 1992; pp 37, 73.
(34) McCafferty, E.; Pravdic, V.; Zettlemoyer, A. C. *Trans. Faraday Soc.* **1970**, *66*, 1920.
(35) Iwauchi, K. *J. Appl. Phys.* **1971**, *10*, 1520.
(36) Bockris, J. O'M.; Reddy, A. K. N. *Modern Electrochemistry*; Plenum Press: New York, 1973; Vol. 2, p 757.
(37) Bockris, J. O'M.; Khan, S. U. M. *Surface Electrochemistry*; Plenum Press: New York, 1993; p 97.
(38) Morimoto, T.; Iwaki, T. *J. Chem. Soc., Faraday Trans. 1* **1987**, *83*, 943.
(39) Iwaki, T.; Morimoto, T. *Langmuir* **1987**, *3*, 282.
(40) Kuwabara, R.; Iwaki, T.; Morimoto, T. *Langmuir* **1987**, *3*, 1059.
(41) Shock, E. L.; Helgeson, H. C. *Geochim. Cosmochim. Acta* **1988**, *52*, 2009.
(42) Shannon, R. D. *J. Appl. Phys.* **1993**, *73*, 348.
(43) Bourikos, K.; Himestra, T.; Van Riemsdijk, W. H. *Langmuir* **2001**, *17*, 749.
(44) Tossell, J. A.; Sahai, N. *Geochim. Cosmochim. Acta* **2000**, *64*, 4097.
(45) Shannon, R. D. *Acta Crystallogr. A* **1976**, *32*, 751.
(46) Wells, A. F. *Structural Inorganic Chemistry*, 4th ed.; Clarendon Press: Oxford, 1975; pp 474, 711.
(47) Soshnikov, L. E.; Urbanovich, S. I.; Kurilovich, N. F. *Phys. Solid State* **1995**, *37*, 1674−1676.
(48) El-Wakkad, S. E. S.; Rizk, H. A. *J. Phys. Chem.* **1957**, *61*, 494−497.
(49) Gonzalez, G.; Saraiva, S. M. *J. Dispersion Sci. Tecnol.* **1994**, *15*, 123−32.
(50) Kosmulski, M. *Langmuir* **1997**, *13*, 6315.
(51) Yamaguchi, T.; Tanaka, Y.; Tanabe, K. *J. Catal.* **1980**, *65*, 442.
(52) Contescu, C.; Jagiello, J.; Schwarz, J. A. *J. Phys. Chem.* **1993**, *97*, 10152.
(53) Vijh, A. K. *Appl. Phys. Commun.* **1994**, *13*, 275.
(54) Butler, M. A.; Ginley, D. S. *J. Electrochem. Soc.* **1978**, *125*, 228.
(55) Burns, R. *Mineralogical Applications of Crystal Field Theory*, 2nd ed.; Cambridge University Press: Cambridge, U.K., 1993; p 338.
(56) Healy, T. W.; Herring, A. P.; Furstenau, D. W. *J. Colloid Interface Sci.* **1966**, *21*, 435.
(57) Stumm, W.; Huang, C. P.; Jenkins, S. R. *Croat. Chem. Acta* **1970**, *42*, 223.
(58) Kanungo, S. B.; Parida, K. M. *J. Colloid Interface Sci.* **1984**, *98*, 252.
(59) Ardizzone S.; Trasatti, S. *Adv. Colloid Interface Sci.* **1996**, *64*, 173.
(60) Kokarev, G. A.; Kolesnikov, V. A.; Gubin, A. F.; Korobanov, A. A. *Elektrokhimiya* **1982**, *18*, 466 (in Russian).
(61) Kleijn, J. M. *Colloids Surf.* **1990**, *51*, 37.
(62) Olhoeft, G. R. In *Physical Properties of Rocks and Minerals*; Touloukian, Y. S., Judd, W. R., Ho, R. F., Eds.; McGraw-Hill: New York, 1981; pp 300−324.
(63) El Shafei, G. M. S. *J. Colloid Interface Sci.* **1996**, *182*, 249.
(64) Goniakowski, J.; Bouette-Russo, S.; Noguera, C. *Surf. Sci.* **1993**, *284*, 315.
(65) Burdett, J. K.; McLarnan, T. J. *Am. Mineral.* **1984**, *69*, 601.
(66) Madden, P. A.; Wilson, M. *Chem. Soc. Rev.* **1996**, *25*, 339.
(67) Burdett, J. K. *Chemical Bonding in Solids*; Oxford University Press: New York, 1995; p 191.
(68) Nortier, P.; Borosy, A. P.; Allavena, M. *J. Phys. Chem. B* **1997**, *101*, 1347.
(69) Pearson, R. G. *J. Am. Chem. Soc.* **1963**, *85*, 3533.
(70) Pearson, R. G. *Inorg. Chem.* **1988**, *27*, 734.
(71) Klopman, G. *J. Am. Chem. Soc.* **1968**, *90*, 223.
(72) Parr, R. G.; Donnelly, R. A.; Levy, M.; Palke, W. E. *J. Chem. Phys.* **1978**, *68*, 3801.
(73) Parr, R. G. *J. Am. Chem. Soc.* **1983**, *105*, 7512.
(74) Jorgensen, C. K. *Struct. Bonding* **1966**, *1*, 234.
(75) Jorgensen, C. K. *Struct. Bonding* **1967**, *3*, 106.
(76) Williams, R. J. P.; Hale, J. D. *Struct. Bonding* **1966**, *1*, 249.
(77) Hancock, R. D.; Martel, A. R. *J. Chem. Educ.* **1996**, *73*, 654.
(78) Gibbs, G. V. In *Silica: Physical Behavior, Geochemistry and Materials Applications*; Heaney, P. J., Prewitt, C. T., Gibbs, G. V., Eds.; Reviews in Mineralogy 29; Mineralogical Society of America: Washington, DC, 1994; pp 360−363.
(79) Rustad, J. R.; Dixon, D. A.; Kubicki, J. D.; Felmy, A. R. *J. Phys. Chem. A* **2000**, *104*, 4051.
(80) Healy, T. W.; Furstenau, D. W. *J. Colloid Interface Sci.* **1965**, *20*, 376.
(81) Henry, M.; Jolivet, J. P.; Livage J. *Struct. Bonding* **1992**, *77*, 153.
(82) Bebie, J.; Schoonen, M. A. A.; Fuhrmann, M.; Storngin, D. R. *Geochim. Cosmochim. Acta* **1998**, *62*, 633.
(83) Wyckoff, R. W. G. *Crystal Structures*; John Wiley: New York, 1963; Vol. 3, p 31.

Received for review April 12, 2001. Revised manuscript received August 14, 2001. Accepted October 22, 2001.

ES010850U